JOURNAL OF NEUROPHYSIOLOGY
Vol. 54, No. 4, October 1985. *Printed in U.S.A.*

Visually Induced Adaptive Changes in Primate Saccadic Oculomotor Control Signals

L. M. OPTICAN AND F. A. MILES

Laboratory of Sensorimotor Research, National Eye Institute; and Laboratory of Neurophysiology, National Institute of Mental Health, National Institutes of Health, Bethesda, Maryland 20892

SUMMARY AND CONCLUSIONS

1. Saccades are the rapid eye movements used to change visual fixation. Normal saccades end abruptly with very little postsaccadic ocular drift, but acute ocular motor deficits can cause the eyes to drift appreciably after a saccade. Previous studies in both patients and monkeys with peripheral ocular motor deficits have demonstrated that the brain can suppress such postsaccadic drifts. Ocular drift might be suppressed in response to visual and/or proprioceptive feedback of position and/or velocity errors. This study attempts to characterize the adaptive mechanism for suppression of postsaccadic drift.

2. The responses of seven rhesus monkeys were studied to postsaccadic retinal slip induced by horizontal exponential movements of a full-field stimulus. After several hours of saccade-related retinal image slip, the eye movements of the monkeys developed a zero-latency, compensatory postsaccadic ocular drift. This ocular drift was still evident in the dark, although smaller (typically 15% of the amplitude of the antecedent saccade, up to a maximum drift of 8°). Retinal slip alone, without a net displacement of the image, was sufficient to elicit these adaptive changes, and compensation for leftward and rightward saccades was independent.

3. It took several days to complete adaptation, but recovery (in the light) was much quicker. The decay of this adaptation in darkness was very slow; after 3 days the ocular drift was reduced by <50%. The time constants of single exponential curve fits to adaptation time courses of data from five animals were 35 h for acquisition, 4 h for recovery, and at least 40 h for decay in darkness.

4. Descriptions of the central innervation for a saccade are usually simplified to only two components: a pulse and a step. It has been hypothesized that suppression of pathological postsaccadic drift is achieved by adjusting the ratio of the pulse to the step of innervation (19, 26). However, we show that the time constant of the ocular drift is influenced by the time constant of the adapting stimulus, which cannot be explained by the simple pulse-step model of saccadic innervation.

5. A more realistic representation of the saccadic innervation has three components: a pulse, an exponential slide, and a step. Normal saccades were accurately simulated by a fourth-order, linear model of the ocular motor plant driven by such a pulse-slide-step combination. Saccades made after prolonged exposure to optically induced retinal image slip could also be simulated by properly adjusting the slide and step components. Thus we hypothesize that adaptive control of the gain of the step, and of both the gain and the time constant of the slide, is required to suppress postsaccadic ocular drift.

INTRODUCTION

Visual acuity begins to decline as images slip across the retina at more than a few degrees per second. It is therefore desirable that the eyes be reasonably stable during fixation of the stationary world. Fixation is changed with very rapid eye movements, called saccades, minimizing the period of poor visual acuity. However, the nervous system is not always successful in reestablishing fixation immediately after a saccade; occasionally there is an accompanying exponential drift of small amplitude, either onward or backward (3, 40). In normal subjects these postsaccadic drifts are usually too small to compromise acuity, but

they can be quite pronounced in patients with ocular motor nerve palsies (1, 19) and in some patients with cerebellar disease (20).

Kommerell et al. (19) demonstrated the existence of a long-term adaptive mechanism that operates to reduce this postsaccadic drift. Using human patients with abducens nerve palsies that result in hypometria and postsaccadic drift in one eye, they showed that the amount of saccadic dysmetria and postsaccadic drift could be altered by monocular patching. When the normal eye was patched for several days its saccades became hypermetric (went beyond the target) and were followed by drift. Switching the patch for 3 days, so that the normal eye was viewing, resulted in recovery of that eye, i.e., the saccades made by the normal eye were of normal amplitude and had no postsaccadic drift. Abel et al. (1) found similar adaptive changes in a patient with an ocular motor nerve palsy. In addition, they followed the time course of the saccadic gains in their patient after patching one eye. When the affected eye alone was viewing, the saccadic gain increased with a time constant of 0.85 days, and when the unaffected eye was viewing the gain recovered with a time constant of 1.54 days.

The rapid part of a saccade is due largely to a brief, high-frequency burst of innervation, or pulse, and the final eye position is determined by a tonic level of innervation, or step (31). Kommerell et al. (19) hypothesized that saccadic adaptation was achieved by altering the pulse and step of innervation. Drift suppression would then depend upon adjusting the ratio of the pulse to the step. Optican and Robinson (26) were able to show, with ablation studies, that the pulse and step gains were independent and that their control depended on different parts of the cerebellum. These workers tenectomized the horizontal recti muscles (excised their distal ends) in one eye of monkeys and allowed the stumps to reattach to the globe. This made saccades in the operated eye hypometric (too small) and induced an exponential drift back (in the direction opposite to that of the antecedent saccade). By patching one eye or the other they were able to study adaptive changes in saccadic gains. The amplitude of the saccade was measured at the end of the initial rapid phase to provide an estimate of the pulse gain and after the achievement of a steady-state position to provide an estimate of the step gain. Both gains were found to change with the same time course, increasing with a time constant of about 1 day, and decreasing with a time constant of about ½ day. Total cerebellectomy resulted in saccadic hypermetria and postsaccadic ocular drift and abolished control of both pulse and step gains. Ablations of the midline cerebellar vermis resulted in saccadic hypermetria and destroyed the animals' ability to adjust their pulse gain, but left intact their ability to adjust their step gain. The gain of the step was not adjusted to match the target displacement, but was always matched to the antecedent pulse of innervation, so that postsaccadic ocular drift was always suppressed despite steady-state position errors. Bilateral flocculectomies in monkeys have been shown to abolish the ability to suppress postsaccadic ocular drift, presumably by destroying the control of the step gain (27).

While the existence of the drift-suppression mechanism is now well established, the mechanism by which the system senses errors and implements corrective adjustments is not known. Two different afferent systems could be used to report the presence of ocular drift. Since the world is stationary, any postsaccadic ocular drift would result in full-field retinal slip, which could therefore be used to indicate the presence of such ocular drift. The assessment of ocular drift might also be made from muscle proprioceptive afference. The extraocular muscles contain many proprioceptors, and these are known to project into the paravermal cerebellum (on which the pulse gain is dependent) over pathways with a short latency in cats (5, 10, 37). Extraocular afferents have also been shown to project to the flocculus (on which the step gain is dependent) in rabbits (22). Since the previously mentioned studies of saccadic adaptation were done on patients with ocular motor nerve palsies or in animals with tenectomized muscles, it is difficult to determine the extent to which proprioception plays a role in drift suppression. It is also not known how the adaptive control of saccade amplitude, presumably effected by changing the gain of the brain's estimate of the target's position (23), interacts with the adaptive mechanism for drift suppression. Both mechanisms appear to have similar time courses of many hours in abnormal subjects (1, 26). However, another, faster adaptive mechanism that makes a parametric adjustment in saccadic size within a few minutes has also been

demonstrated in normal human subjects (8, 14, 41).

The present study was undertaken to characterize the contribution of retinal slip to the adaptive mechanism responsible for minimizing postsaccadic ocular drift. The visual experience of patients with extraocular muscle palsies (1, 19) and monkeys after tenectomies (26), i.e., exponential slips after saccades, was reproduced as closely as possible in these experiments in an attempt to stimulate the same gradual adaptive mechanism for drift suppression. Monkeys with intact extraocular muscles experienced optically imposed, full-field, exponential postsaccadic retinal slip. The monkeys responded to this retinal slip just as if it had been caused by pathological ocular drift; changes in saccadic innervation led to the development of a postsaccadic ocular drift that reduced the optically imposed postsaccadic retinal slip. Unexpectedly, the time constant of this ocular drift was dependent on the time constant of the adapting image's drift. Hence these studies show that, in addition to the amplitude of the drift, the time constant of the drift is also under adaptive control. These data lead to the proposal of a new model of the final common path, the brain stem network and ocular motor plant, which is common to all ocular motor systems. The new hypothesis accurately models both normal and adapted saccades, allowing for the suppression of postsaccadic ocular drift. A preliminary report of some of these results has been presented (25).

METHODS

Eye movements were recorded from seven adult rhesus monkeys (*Macaca mulatta*) before, during, and after they experienced optically imposed postsaccadic retinal image slip. All animals had previously been trained to fixate small lights for a liquid reward. Each animal was implanted with a head holder and a scleral search coil (15), using aseptic surgical procedures, while under pentobarbital sodium anesthesia. During the experiments animals were seated in a plastic chair, with their heads fixed, facing a translucent screen subtending 100° in both the horizontal and vertical direction at a distance of 29 cm. Highly textured, colored images were projected onto the back of the screen and were moved by a mirror galvanometer system under computer control. This arrangement was used to drift the scene with an exponential time course after every spontaneous saccade, thereby simulating the visual events associated with postsaccadic ocular drift.

Motion of the projected image was controlled by a PDP-11/34 computer driving a servo-controlled mirror galvanometer (General Scanning Corp. CCX-101 servo and G300-PD motor). The bandwidth of the scanner was ~100 Hz, and the control signal had a range of 100° of image motion with a resolution of 1 part in 4,096. Three signals, horizontal and vertical eye position and the transducer output of the mirror galvanometer, were low-pass filtered (−3 dB at 240 Hz) and digitized with a 12-bit analog-to-digital converter sampling 1,000 times per second.

Eye movements were recorded monocularly with the magnetic-field/search-coil technique (24, 30). A relative calibration was routinely made by moving the image with a saw-tooth waveform (constant-velocity slow phases at 10 deg/s, interrupted by 10-ms resets) and assuming that the maximum optokinetically induced eye velocity matched the velocity of the projected scene. Absolute calibrations for testing saccadic accuracy were made by having the monkey make saccades to targets at 20° eccentricity left, right, up, and down.

Adaptation paradigm

The adaptation paradigm was designed to elicit a change in the pulse-step ratio of saccadic innervation. While the animal faced the textured image and made saccadic eye movements spontaneously, the computer detected the saccades on the basis of velocity and duration criteria (2). At the end of each saccade (which could be determined with an accuracy of a few milliseconds by waiting for the eye velocity to fall below 12% of its peak value) the computer made the projected image move horizontally across the screen. There was a 5-ms latency between the computer command and the mirror movement. Since the computer detected a low eye velocity, and not the true end of the saccade, the movement of the image usually began within a few milliseconds of the actual end of the saccade. Generally, an exponential waveform with a 50-ms time constant was used. This value was chosen to be near that of the ocular drift found in a previous study of lesioned animals where adaptation was observed (26). Some experiments were done with exponential drifts having other time constants (25 and 100 ms), and in one experiment the scene was displaced abruptly. The amplitude of the image slip was always 50% of the amplitude of the horizontal component of the antecedent saccade. In some experiments the slip was onward, in the direction of the antecedent eye movement, and in others it was backward. Animals remained in the apparatus for the several days needed to complete a single experiment. They were given food and water by hand, at regular intervals, until satiated, regardless of their behavior. Animals were kept awake during recording sessions by loud noises. At other times six animals were not artificially aroused. The seventh animal received a liquid reward for making brisk sac-

cades. There was little difference in this animal's adaptive performance.

Latency of the ocular following response to the full-field, exponential slip stimuli was measured with the techniques of Kawano and Miles (16). The eye velocity was digitally differentiated to obtain an acceleration trace. We computed the mean and variance of this acceleration over the period before the stimulus. Onset of ocular drift was defined to be when the eye acceleration exceeded 2 SD from the mean. This was typically at $\sim 100°/s^2$.

Saccadic performance

Sample recordings of saccadic and postsaccadic waveforms were made while the animal was viewing the adapting stimulus and while it was in temporary darkness. For testing saccadic accuracy the eye without the coil was patched, and the animal tracked a spot of light that shifted abruptly among fixed positions at 0, ±5, ±10, ±15 and ±20° along the horizontal meridian. The sequence of the target movements was unpredictable and included various combinations of starting positions and amplitudes.

Data from the first two monkeys were measured by hand from chart paper records. Data from later monkeys were analyzed off-line on a PDP-11/44 computer. Velocities were obtained by digital differentiation, using a Chebyshev optimal nonrecursive linear filter acting as a low-pass filter (−3 dB at 30 Hz) (29). Each saccade was displayed on a video screen, and measurements were made of the beginning and ending positions of the saccades, their peak velocity, and the amplitude and duration of any postsaccadic drift. Time constants of image and ocular drift were estimated by a nonlinear regression technique with linear constraints on the parameters that determined the best fit, in the least-square-error sense, of a single exponential curve to the data (21, 38).

RESULTS

When the full-field image first begins moving after every saccade, the animal responds by tracking it with a delay of ~50–60 ms (cf. Ref. 16). If the lights are turned off after only a few minutes of such experience, the animal's spontaneous saccades in the dark appear normal. After several hours of such experience, however, the monkey begins to show a zero-latency ocular drift after each saccade in the light, and some of this drift persists when the lights are turned off. Our initial concern is entirely with the postsaccadic ocular drifts that persist in the dark (though a later section will consider some of the complex events recorded in the presence of the adapting stimulus in the light).

Optically induced postsaccadic ocular drift in the dark

Figure 1 shows the effect of prolonged exposure to the adaptation paradigm on spontaneous saccades made in the dark. In the normal state of the animal (Fig. 1*A*) the saccadic eye movement ended fairly abruptly and was followed by only a small amplitude drift back. Such small drifts are often present in the light as well as in the dark in the normal state. After several days of experiencing optically imposed retinal slip after every saccade, the eyes developed a drift in the direction of the adapting motion that followed almost immediately after the rapid part of the saccade was over (Fig. 1, *B* and *C*).

Comparing the panels in Fig. 1, we see that the adapted movement looks like a rapid saccade followed by a slow drift. To quantify this adaptive response, eye movements were divided into two parts: an initial rapid component of amplitude P, presumed to reflect a phasic change of innervation, or pulse, and a component of amplitude S that brings the eye to its final position, presumed to reflect a tonic level of innervation, or step. The size of component P is measured from the initial eye position to the inflection point during the deceleration phase of the rapid part of the saccade. The size of component S is measured from the initial eye position to the point where the eye velocity returns to zero.

The amplitude of the postsaccadic ocular drift (S − P) varied with the amplitude of the antecedent saccade. Figure 2 shows data from two monkeys, in which each point indicates the ocular drift following a spontaneous saccade in the dark, after 5 days of adaptation. In both cases the adapting stimulus was an exponential image drift with a time constant of 50 ms and an amplitude that was 50% of the antecedent saccade's. Circles show drifts from monkey OV, after adapting to a stimulus that drifted backward; plus symbols show drifts from monkey UL, after adapting to a stimulus that drifted onward; the straight lines are least-squares regressions of ocular drift on saccadic amplitude for amplitudes less than about 25° (for OV: slope = −0.17, intercept = −0.54°, $r = -0.97$; for UL: slope = 0.12, intercept = 0.10°, $r = 0.95$). For larger saccades the points tend to fall off the regression line, indicating the presence of an amplitude saturation for ocular drift. Indeed, ocular drifts in the dark

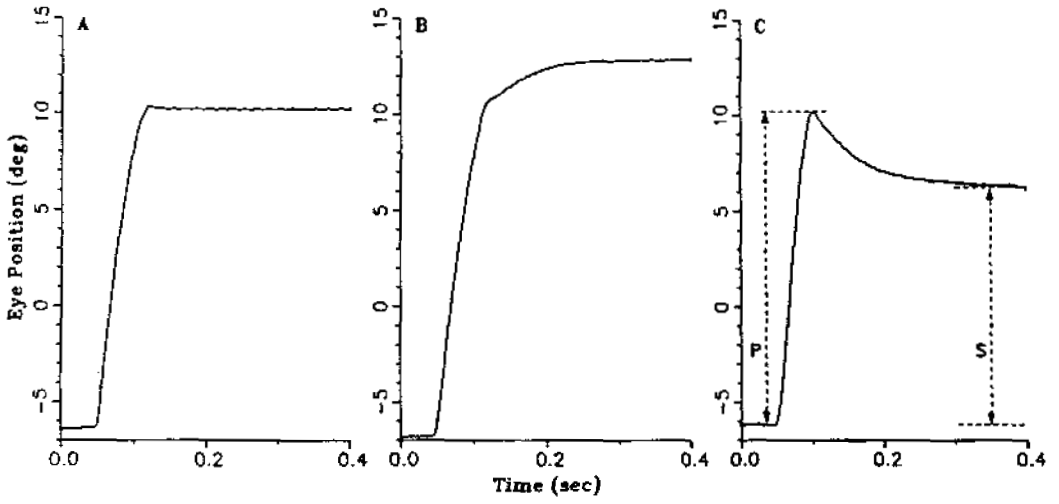

FIG. 1. Optically induced postsaccadic ocular drift persists in the dark. *A*: normal spontaneous saccade in the dark. Note small amount of drift back at the end of the rapid portion of the saccade. Spontaneous saccade in the dark after several days of exposure to an onward (*B*) and backward (*C*) exponential drift that followed every saccade. The saccade in the adapted state is followed by a zero-latency drift. To quantify the amount of ocular drift, the amplitude of the rapid part of the saccade (P) and the final position of the movement (S) are measured from the saccade's starting point. The portion P is called the saccade, and the portion (S − P) is called the postsaccadic ocular drift.

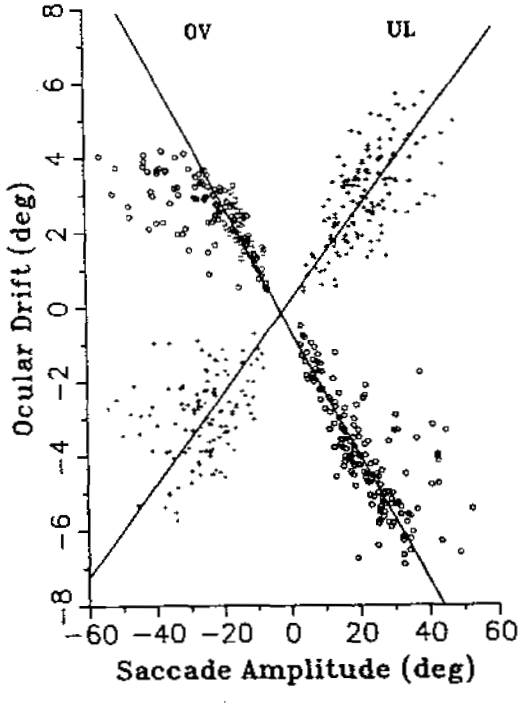

FIG. 2. The amplitude of ocular drift in the dark is proportional to the amplitude of the antecedent saccade. Ocular drift amplitudes were measured in monkey OV (with backward drifts, *circles*) and in monkey UL (with onward drifts, *plus symbols*). The *solid lines* are the regressions of ocular drift amplitude on saccade amplitude for saccades <25°.

with amplitudes >8° were not seen in any monkey.

The amount of drift was also expressed as a fraction of the pulse amplitude, (P − S)/P, and will be referred to as the pulse-step mismatch (psm). The relationship between the pulse and step components was also expressed by the fraction (P/S), called the pulse-step ratio (psr). The almost linear relationship between the amplitude of the ocular drift and its antecedent saccade suggests the presence of a parametric adjustment (with saturation), and supports the use of a single number, such as the psm or psr, to characterize the saccadic waveform in the presence of ocular drift. Table 1 shows the psm (in %) for four monkeys. The visual scene was made to slip either backward or onward 50% of the amplitude of the antecedent saccade. In each case the monkey, in response to the retinal slip, developed a postsaccadic ocular drift that was in the adaptive direction.

The amount of the postsaccadic drift in the dark was always less than that in the light. As a typical example, in monkey UL, the psm after 6 days of adaptation (to an exponential drift with 50% the amplitude of the antecedent saccade and a time constant of 50 ms) was 24.3 ± 1.2% (SE) in the presence of the adapting stimulus, but only 13.6 ± 0.3% in the dark.

TABLE 1. *Pulse-step mismatch of spontaneous saccades made in the dark*

Monkey	Normal, %	Adapted, %	
		Backward slip	Onward slip
OV	1.6 ± 0.2 (57)	17.5 ± 0.5 (107)	−17.3 ± 0.6 (84)
UL	2.5 ± 0.2 (108)	7.7 ± 0.5 (52)	−13.6 ± 0.3 (329)
RO	1.1 ± 0.2 (38)		−11.0 ± 0.8 (71)
QU	1.5 ± 0.2 (75)		−20.6 ± 0.6 (73)

Adapted state was induced by several days of exposure to an image slip whose amplitude was 50% of the amplitude of the antecedent saccade and which drifted exponentially with a time constant of 50 ms. Values are means ± 1 SE (n).

Time constant of ocular drift

The time constant of the ocular drift associated with an adapting stimulus of a given time constant was fairly consistent in the same animal on different days, although there were small differences between animals. The average time constant of ocular drift in four animals measured in nine separate experiments was 68.8 ms (SD = 10.8) when the adapting stimulus had a time constant of 50 ms. The time constants within this group ranged from 51.0 ± 1.4 (SE) (n = 84) to 87.1 ± 3.5 ms (n = 61); analysis of variance showed that the group was not homogeneous (F-test, $P < 0.01$), and hence the time constants among monkeys were significantly different.

These significant differences suggested that the time constant of the ocular drift might be an idiosyncrasy of the animal and independent of the time constant of the adapting stimulus. To test this hypothesis, the effect of varying the time constant of the exponential image drift used for adaptation was examined in two monkeys. In three separate experiments the time constant of image motion was either 25, 50, or 100 ms. Figure 3 shows that there was a strong correlation between the time constant of the ocular drift and that of the image drift used to adapt the animals. After adaptation the psm was about 15% in all experiments, and there was no marked difference in the acquisition time at the different adapting time constants. Nor was there any correlation between saccade amplitude and the time constant of the ocular drift; for two monkeys (OV and LF), with the three adapting image-drift time constants, the average of the absolute values of the correlation coefficients was 0.20 ± 0.22 (SD) (ranging from 0.003 to 0.500). Regression of the ocular-drift time constant on the image-drift time constant gives a line with slope 0.70 and intercept 19.61 ms (correlation coefficient 0.99) for the data of both monkeys. Hence the time constant of the ocular drift in the dark was dependent on the time constant of the stimulus used in the adaptation paradigm.

Time course of acquisition and recovery

The postsaccadic ocular drifts recorded in the dark develop gradually over time when an

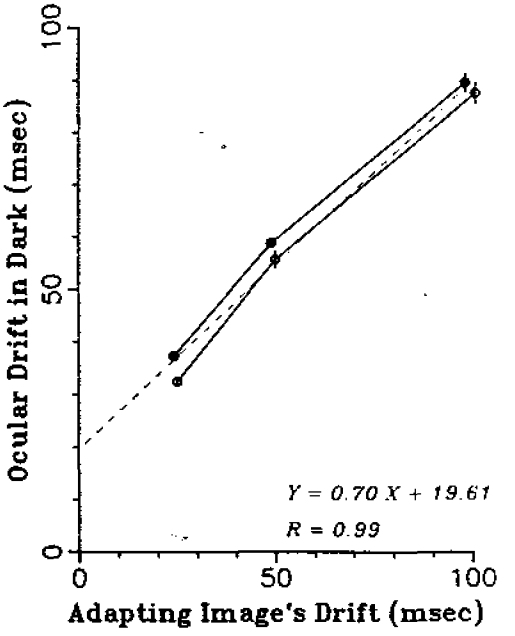

FIG. 3. Time constant of ocular drift measured from spontaneous saccades, made by monkey OV (*open circles*) and LF (*filled circles*) in the dark, depends on the time constant of the adapting stimulus. *Vertical* and *horizontal bars* are ±1 SE. *Dotted line* is from linear regression. Time constants of image drift are an average of 15, and time constants of ocular drift are averages of at least 60 nonlinear regression estimates (see METHODS). The correlation between ocular and image time constants is statistically significant ($P < 0.001$). [Actual time constants of image drift for monkey OV were 25.0 ± 0.1 (SE), 50.1 ± 0.1, and 101.0 ± 0.2; for monkey LF they were 24.1 ± 0.1, 49.1 ± 0.3, and 98.5 ± 0.5.]

animal is continually exposed to optically imposed postsaccadic slip. Figure 4 shows a typical time course for the adaptive change in the psm in monkey UL. The animal was adapted for 6 days to an exponential image drift (with a 50-ms time constant) that slipped onward in one experiment (open circles) and backward in another (filled circles). At the end of the 6th day the image motion was stopped, and the animal was allowed to recover while viewing the (now stationary) image. The recovery phase was much shorter than the acquisition phase, regardless of the direction of the gain change, even though the visual stimulus was the same in the two cases, and the monkey generated saccades at a similar rate. An effort was made to fit a single exponential function to the acquisition and recovery time courses. This was not possible in the acquisition phase when the step gain was increasing (where a dashed line connects the points); the gain appeared to increase in two stages for this monkey. When the step gain was decreasing, the acquisition phase had a time constant of 30.4 ± 6.4 h (SE). Both recovery phases were well fit by exponential functions. The time constant for recovery from a gain decrease was 5.4 ± 1.0 h, and that for a recovery from a gain increase was 4.7 ± 1.2 h. Time course data were also plotted using the number of saccades, instead of the elapsed time, as the independent variable. Essentially no difference in the smoothness or form of the curves resulted from expressing the data in this way.

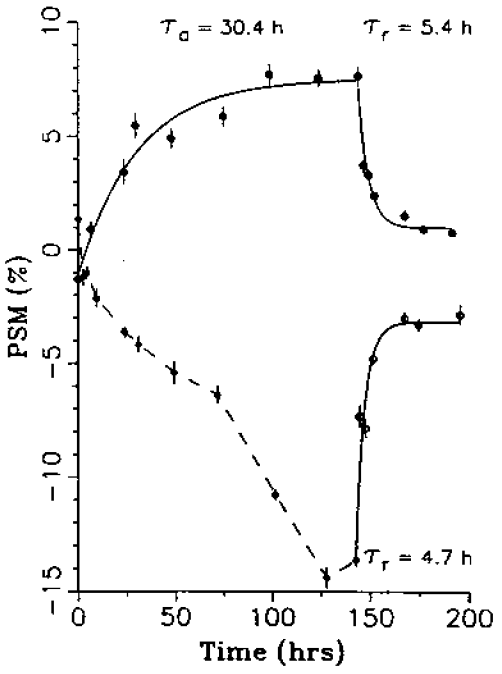

FIG. 4. Time course of adaptation in monkey UL. At time zero the animal was presented with exponential image slip that was 50% of the amplitude of the antecedent saccade. In one experiment the image drifted in the same direction as the antecedent saccade (*open circles*), and in the other the image drifted backward (*filled circles*). *Vertical bars* are ±1 SE.

The time course of the acquisition of an adapted gain was studied in five experiments on four monkeys. The time course of the recovery from the adapted state was studied in four experiments in three monkeys. In all the animals the change over time of the psm was usually smooth, although, as in Fig. 4, often one change was not well fit by a single exponential (but this could be the acquisition of either an increased or a decreased psm). There were no systematic differences across monkeys whether the gains were increasing or decreasing, or between gains for leftward or rightward movements. While there were differences in the time constants for leftward and rightward adaptation, this varied from monkey to monkey. In only two cases (out of 8) were the time constants of acquisition shorter than the time constants of recovery, and then only for one direction; combining leftward and rightward data to give a single time constant always gave an acquisition time constant that was larger than the recovery time constant. A characterization of the overall performance in all the monkeys was obtained by normalizing the psm so that the maximum value during each phase (acquisition or recovery) in each monkey was +1.0. All the normalized psm values from each monkey were divided into acquisition and recovery groups. The recovery values were time shifted so that all the recovery phases started at 167 h. Single exponential functions were fitted to all the points in both groups. In Fig. 5 the letters correspond to psm values from each monkey for leftward and rightward saccades. The solid lines are the least-squares best fit to the data of a single exponential function. The time constant of acquisition was 35.1 ± 6.5 h (SE), and that of recovery was 4.1 ± 0.7 h.

Decay of adaptation in darkness

If the postsaccadic ocular drift is to be ascribed to changes in some plastic neural gain elements, one would expect those changes to

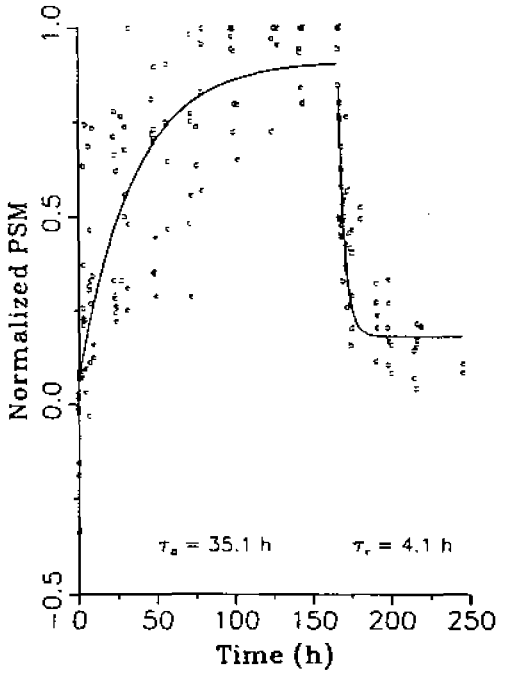

FIG. 5. Time course of adaptation averaged over 5 experiments in 4 monkeys. *Letters* represent individual monkeys. The *curves* represent the best-fit single exponential function to the pooled data.

persist in the dark when there can be no postsaccadic retinal slip. The long-term persistence of the psm was examined by adapting two monkeys (for 4 and 5 days, respectively) and then placing them in complete darkness. The amount of postsaccadic ocular drift associated with spontaneous saccades in the dark was measured by pooling the psm values for rightward and leftward data for each monkey (normalized to the value at time zero).

Figure 6 shows the pooled values (open circles are monkey OV, filled circles are monkey UL). Despite the variability of the data, reflected in the large standard errors, it is clear that the decay of the psm in darkness is less rapid than either the acquisition or recovery phases. For comparison with the time constants in Fig. 5, exponentials were fitted to the data in Fig. 6 as well. Fitting a single exponential gives a very long time constant for decay to zero [180 ± 31 h (SE), solid line]. As expected, fitting a single exponential that decays to a nonzero asymptote gives a shorter time constant (42 ± 32 h, with an asymptote of 0.53, dashed line), but one that is still longer than that for either acquisition or recovery. While the decay in the dark is not a simple process that can be well fit by a single exponential, the psm clearly does not go away rapidly in the dark, and there is considerable residual psm; even after three days in darkness both animals still retain >50% of their adaptation.

Directional selectivity

In all of these experiments the image drifted only in the horizontal plane, and ocular drift developed only in that plane. One experiment was performed (with monkey OV) to further demonstrate the directional specificity of the visually induced adaptive response. In this experiment the image was made to move onward after rightward saccades, and backward after leftward saccades. Thus, the optical drift was always in the same direction, so that the size of the step of neural innervation relative to

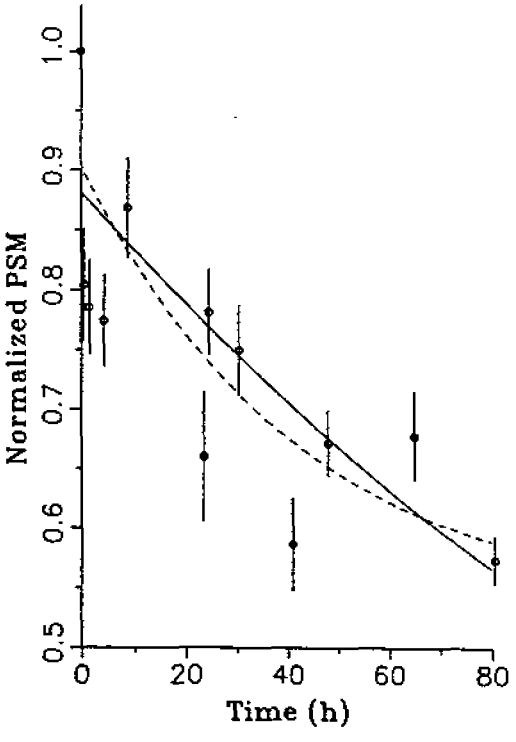

FIG. 6. Decay of adaptation in darkness. After adapting to exponential image slip, 2 monkeys were kept in complete darkness for several days. The values are pooled for each of 2 monkeys for leftward and rightward movements (*open circles* from monkey OV, *filled circles* from UL). *Vertical bars* are ±1 SE. The *solid curve* is the best-fit exponential (time constant = 180 ± 31 h) decaying to zero. The *dashed line* is the best-fit exponential with an asymptote of 0.53 (time constant of 42 ± 32 h).

the pulse was required to increase for rightward movements and decrease for leftward movements. This is exactly what happened, the psr being appropriate for the direction of the antecedent saccade and the direction of adapting image motion: The rightward psm was −9.1% (SE = 0.3, n = 116), while the leftward psm was +9.0% (SE = 0.2, n = 130).

Displacement vs. drift

An exponential pattern of image motion induces both slip and displacement of the retinal image. Several other patterns of image motion were used to study the adaptive mechanism. Prolonged exposure to step displacements (duration of 5–8 ms) in the same direction as the antecedent saccade did not elicit postsaccadic ocular drift; after several days of viewing step displacements that were 50% of the amplitude of the antecedent saccade, eye movements still ended abruptly. Hence displacement alone of the image on the retina is not sufficient to elicit postsaccadic ocular drift. Step displacements and exponential drifts were combined to give an image slip without net image displacement; at the end of a saccade the image stepped away by 50% of the amplitude of the antecedent saccade, then drifted back exponentially to its original position with a time constant of 50 ms. The response of the monkey to this step-back exponential was qualitatively identical to the response to the simple exponential image motion; the psm in the dark, after 3 days of adaptation, was −12% (SE = 0.4, n = 113), while after 3 days of adaptation to the simple exponential it was −17% (SE = 0.6, n = 84) in the same monkey. Thus, optically imposed postsaccadic retinal slip alone, without net retinal image displacement, is sufficient to elicit postsaccadic adaptation.

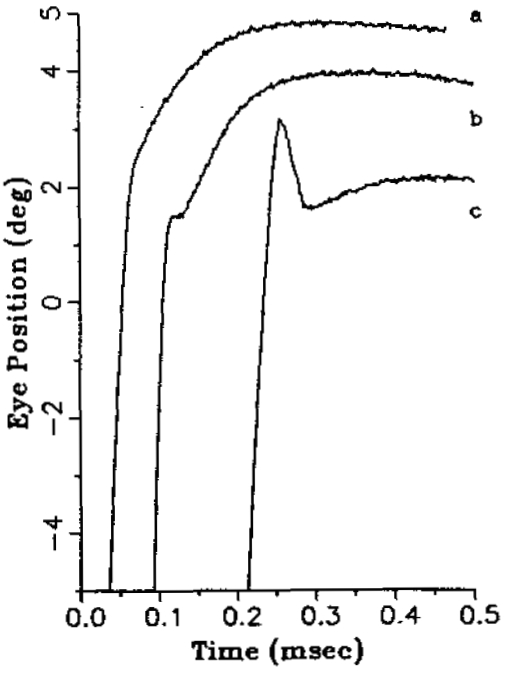

FIG. 7. Representative transition waveforms from saccade to ocular drift in spontaneous saccades in the dark. Eye movements were shifted and their beginnings removed. *a*: the drift begins immediately after the pulse-driven part of the saccade is over. *b*: there is a short period (~10 ms) of zero or low velocity before the drift. *c*: a small backward saccade, or dynamic overshoot, precedes the drift. All monkeys show this spectrum of response waveforms. Which form predominates varies with the monkey and the direction of the saccade.

TABLE 2. *Latency of ocular drift following spontaneous saccades in the dark*

Monkey	Normal	Adapted
OV	3.6 ± 0.4 (51)	3.4 ± 0.2 (107)
UL	6.2 ± 0.4 (108)	5.4 ± 0.2 (329)
RO	4.8 ± 0.8 (38)	4.6 ± 0.5 (71)
QU	3.3 ± 0.3 (75)	2.4 ± 0.1 (73)

Even normal saccades often have small ocular drifts. There is very little difference in the latency from the end of the saccade to the onset of drift between the normal and adapted states. Values are mean times in milliseconds ± 1 SE (n).

Time of onset of postsaccadic ocular drift

In the normal state, before adaptation, the exponential image drift gave rise to an ocular following response. The latency of this response, averaged over two experiments in each of two monkeys, was 56.7 ± 6.6 ms (SD). After several days of adaptation, the animals showed postsaccadic ocular drifts that had much shorter latencies and persisted in the dark. Figure 7 shows examples of the endings of eye movements made in the dark that resulted from adaptation to exponential image slip for several days, selected for their range of postsaccadic ocular drift onset times.

Zero-latency drifts, such as in Fig. 7*a*, represent only one end of a spectrum of latencies. Sometimes there is a short period between the end of the saccade and the beginning of the drift (Fig. 7*b*). In other cases the initial saccade will be followed by a dynamic overshoot (a small, backward saccade) before the drift begins (Fig. 7*c*). Which pattern predominates

varies from one monkey to the next and also depends on the direction of the antecedent saccade. The pattern in Fig. 7*c* was the most rare, occurring ~1% of the time in the dark. Table 2 shows the average latency in the dark to the onset of ocular drift in different monkeys. Ideally, in the normal state in the dark there should be no postsaccadic drift, and hence the latency measurement would be zero. The values for the latency in the animal's normal state in Table 2, however, reflect the fact that even many normal saccades are accompanied by small drifts. Also, there is a systematic error introduced by the method for determining the end of the pulse-driven part of the saccade and the beginning of the ocular drift, which limits the minimum measurable latency to ~2 ms. Clearly there is no significant change in drift latencies, measured in the dark, caused by adaptation.

Effect of adaptation on rapid component dynamics

The amplitude-peak velocity relationships of the initial rapid component of saccadic eye movements were not affected by the adaptation paradigm. Figure 8 shows examples of the amplitude-peak velocity relationship, often

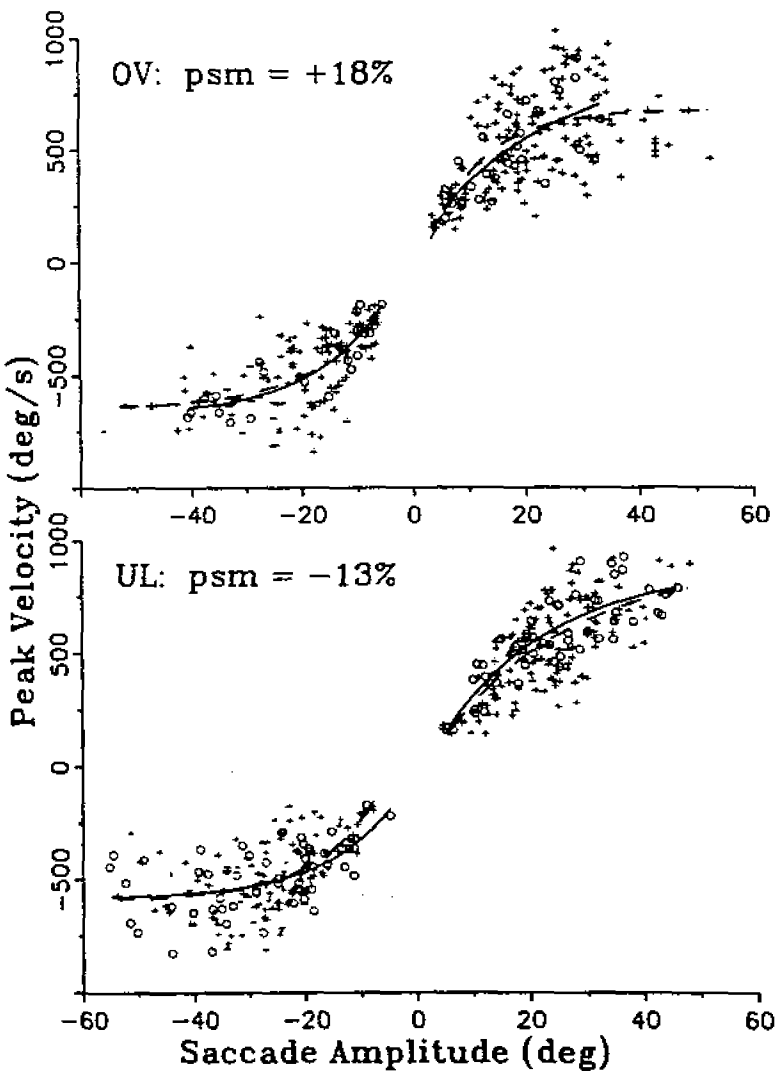

FIG. 8. Main sequence (amplitude-peak velocity relationship of the horizontal component of saccades) was the same for spontaneous saccades in the dark made in the normal (*circles*) and adapted (*plus symbols*) states.

referred to as the *main sequence* (2), obtained in the dark from two monkeys. Abscissa and ordinate values refer to the horizontal component of spontaneous saccades. Since the vertical component of saccades was not altered by this adaptation paradigm, we assume that any effect of oblique saccades on this main sequence would be the same in both the adapted and unadapted states. The circles are the values before adaptation, and the plus symbols are the values after 5 days of adaptation to a 50-ms time constant, exponential image motion that drifted 50% of the amplitude of the antecedent saccade. In Fig. 8, top, the data for monkey OV are shown before and after adaptation to backward image slip. In the adapted state the monkey's psm was +17.5% (SE = 0.5, n = 107). In the bottom part of Fig. 8, the data for monkey UL are shown before and after adaptation to onward image slip. In the adapted state the monkey's psm was −12.8% (SE = 0.3, n = 250). These mismatches were typical of those seen in our experiments.

Even the largest saccades, up to 50° in amplitude, still fell on the same main sequence. The amplitude-peak velocity main sequence can be characterized by a single exponential. The curves are the best-fit exponentials to the data values from the normal (solid) and adapted (dashed) states. The parameters of this exponential fit were compared for leftward and rightward movements by each monkey in both the adapted and normal states. There was no significant difference between the values in these two states (large sample test for difference of means could not reject the hypothesis of equal values even at the 70% confidence level). Parameters of these exponential fits are given in Table 3.

While the mean amplitude-peak velocity relationship did not change, there is clearly a wider range of velocities for a given amplitude in the adapted state when the ocular drift is backward (Fig. 8*A*). From looking at the least-upper-bound of this relationship, instead of the mean, it appears that the saccades in the adapted state can be faster than those in the normal state for amplitudes up to ~25°. (This characterization is not affected by the vertical component of oblique saccades, since slowing of the horizontal component will affect the mean, but not the least-upper-bound, of the data.) This increase in the upper limit of peak velocities for a given amplitude is presumed to be due to the fact that decreasing the step of innervation (to cause a drift back) subtracts a small amount from the portion of the saccade we call pulse-driven (the pulse is actually made up of a burst from the pulse generator and the ramp part of the ramp-step from the neural integrator, see below). Hence the pulse-driven saccadic amplitude is actually a little less than the amplitude programmed by the pulse-generator. The effect of this underestimate of saccade amplitude is to shift the amplitude-peak velocity relationship so that saccades in the adapted state (with backward drift) have larger velocities than normal saccades. Hence the asymptote for large amplitudes will remain the same, but the least-upper-bound will increase for small saccades.

TABLE 3. *Peak-velocity vs. amplitude relationship for monkeys OV and UL in the normal and adapted states (cf. Fig. 8)*

	K, deg/s	A, deg	V_m, deg/s
OV			
Normal			
R	−670 ± 406	23.5 ± 24.8	912 ± 434
L	487 ± 74	13.4 ± 7.5	−682 ± 88
Adapted			
R	−575 ± 57	9.5 ± 2.3	679 ± 36
L	398 ± 43	13.3 ± 3.9	−649 ± 43
Combined			
R	−579 ± 49	10.3 ± 2.3	688 ± 37
L	434 ± 38	13.3 ± 3.4	−654 ± 39
UL			
Normal			
R	−716 ± 92	19.8 ± 7.2	881 ± 112
L	401 ± 88	12.6 ± 5.4	−588 ± 45
Adapted			
R	−794 ± 111	23.0 ± 8.0	906 ± 136
L	440 ± 53	11.1 ± 3.4	−596 ± 41
Combined			
R	−794 ± 83	22.9 ± 6.1	914 ± 102
L	508 ± 60	11.9 ± 2.9	−596 ± 31

The curves are the least-squares best fit (21, 38) of a single exponential: $K \exp(-a/A) + V_m$ where a is the amplitude of the saccade, K is the slope constant, A is the angle constant, and V_m is the peak velocity asymptote. Curves were fit for saccades in both the rightward (R) and leftward (L) directions. The curves in the normal and adapted states were so similar that a single curve was also fit to the combination of the normal and adapted data sets for each monkey (see text). Each parameter is given ± 1 SE.

Effect of adaptation on pulse gain

To determine whether prolonged viewing of the exponential-drift stimulus would cause any change in the amplitude of the rapid com-

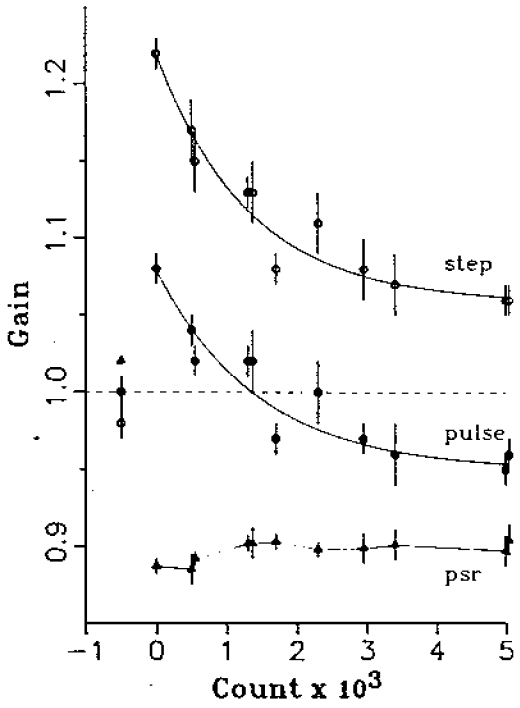

FIG. 9. Adaptation to amplitude dysmetria. Monkey UL was adapted for 3 days to a stimulus that drifted onward. The normal values of the pulse (*filled circles*) and step (*open circles*) gains, and their ratio (*triangles*) is shown at −0.5 on the *abscissa*. After adaptation, the pulse and step gains are raised (and the pulse-step ratio, psr, is lowered). In a spot-tracking task, where the monkey is rewarded for rapidly acquiring the target, the gain of the pulse and step are decreased until a slight hypometria of the pulse is restored. This happens with an exponential time course with a time constant of ~2 h. Since the gain change is in response to the saccades, however, the data is plotted versus total number of saccades since the beginning of the behavioral task.

ponents of saccadic eye movements, an animal that had been adapted for 3 days was examined on the saccadic tracking test. Figure 9 shows the pulse and step gains measured in monkey UL from responses to the movement of a spot target. (The pulse gain is the ratio of the amplitude of the pulse-driven part of the saccade to the initial distance to the target. The step gain is the ratio of the final amplitude of the eye movement to the initial distance to the target.) The step gain is indicated by open circles, the pulse gain by filled circles, and the pulse-step ratio (psr) by triangles. The values for these variables in the preadapted state are indicated by symbols at −0.5 on the abscissa. Note that the abscissa has units of thousands of saccades to facilitate easy comparison with the rapid saccadic amplitude changes seen in human subjects in psychophysical tests (8, 14).

The adaptation paradigm was designed to induce the monkey to adjust the size of the step of saccadic innervation to reduce image slip; however, as the saccade tracking test began it was evident that both the pulse and the step gains were larger than normal. In this test the projected image consisted only of a small spot of light, and the animal was rewarded only for acquiring this (stationary) target rapidly. For the first few movements of the saccade test, the high pulse and step gains drove the eye beyond the target, and the animal had to make corrective saccades. During testing, however, the animal began to decrease the amplitude of the rapid part of the saccade, so that large corrective saccades were no longer necessary; yet the ratio of the rapid component to the step component (psr) did not change. The pulse and step gains were both lowered with a roughly exponential course [step-gain decay constant: 1,308 ± 272 saccades (SE); pulse-gain decay constant: 1,438 ± 436 saccades]. This monkey made ~770 saccades per hour, so the equivalent time constant for the change of both the rapid and step components was ~2 h. This short course is longer than the rapid parametric adjustment of saccadic gain seen in psychophysical experiments on human subjects, which require only a few hundred saccades (8, 14), but is shorter than the several hours or days needed to adapt to pathological retinal slip (1, 19, 26, and Fig. 5 in this study).

DISCUSSION

Persistent postsaccadic retinal slip, induced optically, is sufficient to elicit a postsaccadic ocular drift that is evident even in the dark. When the animal first experiences the full-field exponential retinal slip there is an ocular following response with a latency of only 50–60 ms. This is shorter than the normal smooth-pursuit latency of 130–150 ms (32), and accords with the ultrashort latency ocular following response to full-field ramp movements described by Kawano and Miles (16). After a few hours of exposure to the postsaccadic retinal slip, the animal begins to develop a compensatory, often zero-latency, postsaccadic ocular drift.

This adaptation occurs in animals with intact extraocular muscles, so the ocular drift develops despite the normal proprioceptive signals coming from the extraocular afferents.

We assume that this is an adaptive response from a neural mechanism that normally operates to suppress postsaccadic ocular drift. This adaptive response is not just the uncovering of some intrinsic ocular drift, since it is only in the plane of the stimulus (horizontal), and since the direction of the drift is linked to the antecedent saccade and can be either onward or backward, independently, after rightward or leftward saccades according to the direction of the adapting stimulus. The data obtained with the step, drift, and step-drift adapting waveforms are consistent with the suggestion of Optican and Robinson (26) that the adaptive mechanism regulating postsaccadic ocular drift is sensitive to retinal slip but not retinal displacement. These workers showed that the step gain is adjusted to minimize postsaccadic ocular drift, rather than to match the desired final eye position. The matching of the step to the pulse occurred even when the pulse gain was incorrect, resulting in saccades of normal appearance but inappropriate amplitude.

The gain of the pulse component also increased slightly in response to the exponential slip stimulus (Fig. 9) and would have had the effect of reducing the final position error. The adapted animal in Fig. 9 had a pulse gain of $\sim$1.1 and a step gain of $\sim$1.3. The gain of the step (G_s) seems to be adjusted to match the pulse gain (G_p), as indicated by the almost constant value of the pulse-step ratio (psr) in Fig. 9 and by lesion studies in monkeys (26). Thus we assume we can write the step gain as G_p/psr. To acquire an initial eccentricity of amplitude K, the pulse drives the eye to G_pK, and the step carries the eye to G_pK/psr. The computer would detect the saccade, and move the image another $0.5G_pK$. So, the final image position is at $(1 + 0.5G_p)K$, which gives a position error, e, between intended and final eccentricities of $[1 + (0.5 - 1/\text{psr})G_p]K$. For this example, $e/K = [1 + (0.5 - 1.3/1.1)1.1] = 0.25$. Hence the position error when both the gain of the pulse and step are increased is 25% of the intended eccentricity. If only the step had adapted, (i.e., $G_p = 1$, $G_s = 1/\text{psr} = 1.18$), then the error would have been 32%. The change in pulse gain reduces the error by (32 − 25%) = 7%, hence it contributes an additional 7/32 = 22% to the reduction of the error.

Other studies have shown that changes in pulse gain can occur in man after only a few hundred saccades (8, 14, 41). Such rapid acquisition may be related to conscious strategies, or short time constant, plastic mechanisms. In contrast, the prolonged time course of the changes in ocular drift and their relatively slow decay in the dark are consistent with long-term, plastic alterations in neural components, rather than the short-term deployment of alternative strategies.

Figure 1 demonstrates for the first time that the saccadic system can reduce the amplitude of the step of saccadic innervation below normal. In previous studies (1, 19, 26) saccadic adaptation was always a response to a reduction of the effective strength of the extraocular muscles. Patching one eye or the other could only be used to increase the amplitude of the step, or return it to its normal value. Abel et al. (1) noted that the time constant for increasing the gain in their patient was 0.85 days, whereas the time constant for recovery was 1.54 days. Optican and Robinson (26) gave the time constant for increasing the step gain over three monkeys as $\sim$1 day, with a recovery time constant of $\sim$0.5 days. Since in these experiments the gains could only be made to increase above normal, or decrease to normal during adaptation, it was not clear whether the difference in the time constants between the acquisition and recovery phases was due to the direction of the change or somehow related to the phase (acquisition or recovery) of the adaptive process. In the present set of experiments it was clear that there was an order of magnitude difference in the time constants of the acquisition and recovery phases, regardless of the direction of the actual gain change.

Why the recovery phase, which always returns the step gain to $\sim$1.0, should be faster than the acquisition phase is not known. One hypothesis is that the ocular drift is a pattern of eye movement that the animal learns to emit after every saccade. Then learning the pattern would be slow, but recovery would only require that the pattern no longer be emitted. This explanation is not completely consistent, though, with the continued presence of the drift after prolonged periods in darkness or with the animal's inability to suppress the drift in the saccade test, apparently finding it easier to adapt the pulse gain instead (Fig. 9). Another potentially important factor is that during acquisition, proprioception and vision are in conflict, whereas in recovery they

are in accord. Another hypothesis is that the brain has a very stable set point for the pulse-step ratio that corresponds with minimal postsaccadic ocular drift. To change the pulse-step ratio away from the set point may require the long-term integration of persistent postsaccadic retinal slip. It may be possible to return the ratio to the value specified by the set point by quickly dumping the integrated error. The logical extension of this idea is that the set point itself must be either genetically determined, or under a very slow-acting form of adaptive control. If the latter is the case, patients with chronic disorders (e.g., a 6th nerve palsy) might have a set point that calls for a very high gain. In such a case, it might take longer for the gain to change to the value needed when only the normal eye is viewing and less time for the gain to go back to the raised value when only the paretic eye is viewing (1).

The amplitude of the induced ocular drift is not constant but is roughly proportional to the amplitude of the antecedent saccade. This ratio was typically ~15% for spontaneous saccades in the dark, but the drift amplitude was never >8°. Thus, while the ocular drift would tend to reduce the retinal slip seen just after a saccade, it could not completely cancel it. The adaptive mechanism was unable to fully compensate for the optically induced slip. In animals with peripheral muscle lesions, however, Optican and Robinson (26) found that postsaccadic drift suppression in the light was nearly complete after the operated eye had been viewing for several days. In this study the amplitude of the ocular drift was 15–20%, with a time constant of 40 ms. The imperfect compensation seen in the present study may have been because the optically induced retinal slip (50% of the antecedent saccade in amplitude) exceeded the physiological range in amplitude, or because of a difference in the proprioceptive afference in these two experiments (the animals of Optican and Robinson had surgically altered muscles). The amplitude of the ocular drift is larger in the light in the presence of the adapting stimulus than in the dark, presumably reflecting a contribution from some predictive tracking mechanism. One assumes that such mechanisms are disabled in the dark.

Kommerell et al. (19) hypothesized that the ocular-drift adaptation was simply a readjustment of the ratio of the pulse to the step of saccadic innervation, and thus the ocular drift was a passive consequence of an imbalance between the extraocular muscle forces and the orbital restoring forces at the end of a saccade (19). The time constant of the ocular drift would then reflect the dynamics of the ocular plant after a step input. The plant is not a simple linear system, however, and predicting the time constant of ocular drift is difficult. The dominant time constant of the orbital mechanics in the rhesus monkey is ~200 ms (34, 39). However, perturbations of the neural-muscular system can result in smaller time constants: 11 and 33 ms after oculomotor nerve stimulation (33), 95 ms after monocular forced ductions (18, 36), and 68 ms after stimulation of the medial longitudinal fasciculus (28). Thus it is not a simple matter to predict a priori what the time constant of postsaccadic ocular drift would be if it were determined passively by the mechanics of the orbit.

In our experiments, however, it has been shown for the first time that the time constant of postsaccadic ocular drift is not passively determined but is under adaptive control. The ocular-drift time constant is thus adjusted actively to minimize retinal slip throughout the period of ocular drift. This new result motivates the incorporation of a third adaptable component into the representation of saccadic innervation, and has important consequences for our understanding of how the brain controls eye movements.

A model of the final common path

Experiments on human eye movements led Robinson (31) to represent the plant mechanics as a fourth-order, linear model with one factor in the numerator (called a zero) and four factors (called poles) in the denominator (2 real poles and a complex-pole pair) of its transfer function. A similar transfer function can be used to get a good approximation of our monkeys' eye movements. As pointed out in the original study, the active state tension (and hence the innervation) needed to make a saccade with this fourth-order plant consists of a brief pulse, a small exponential slide, and a final step (31). There is also physiological support for this pulse-slide-step representation of saccadic innervation. Fuchs and Luschei (11) reported and Goldstein (13) quantified the exponential decay of the postsaccadic neural firing rate in abducens nucleus single units of monkeys. Collins et al. (7) recorded with implanted strain gauges during human

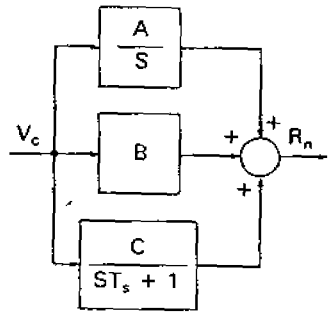

FIG. 10. Block diagram of brain stem network of the final common path for all ocular motor systems. V_c is the velocity command signal coming from the brain stem pulse generator. R_n is the saccadic innervation being sent to the extraocular muscles. The upper block represents the neural integrator, which provides a step with weight A. The middle block provides a pulse with weight B. The first 2 blocks are identical with the final common path previously proposed by Skavenski and Robinson (39). The bottom block is new, and provides an exponentially decaying innervation, or slide, with time constant T_s and weight C.

strabismus surgery and demonstrated exponential decays in the muscle tension after saccades.

The time constant of the neural slide and the time constant of the plant's lead factor (the numerator factor, or zero) have not been measured in the same species. Indeed, in Robinson's original study the value of this plant time constant depended upon certain assumptions about the distribution of stiffness in the model, and was not measured directly. Following Goldstein's approach (13), we propose that the purpose of the neural slide is to compensate for the lead element of the plant dynamics, and thus in our model they are made to have similar time constants. The importance of the slide of innervation to the present study lies in its potential for determining the time constant of postsaccadic ocular drift. We assume that the dynamics of the plant are almost completely compensated for by the dynamics of the brain stem neural network, and that eye velocity is determined solely by the firing rate of the medium lead burst neurons in the pontine reticular formation (6, 12, 17). If the firing rate of the bursters is proportional to eye velocity [neglecting an amplitude nonlinearity (12)], then the overall effect of the final common path must be to mathematically integrate a burst of neuronal discharge encoding eye velocity, thereby producing the eye position (39). Figure 10 shows a simplified block diagram (in Laplace transform notation) of the proposed brain stem neural network. The velocity command (V_c) is passed through three blocks, the sum of whose outputs constitutes the ocular motor control signal (R_n). The velocity command is essentially a brief pulse. The top block represents the neural integrator, with gain A, the output of which is a ramp-step obtained by integrating the input pulse. The middle block represents the direct velocity contribution of the pulse (with gain B), acting as a preemphasis for the sluggish plant. The bottom block represents a low-pass filter with time constant T_s and DC gain C. The output of this block is a low-pass filtered version of the pulse. Combining the output of these three branches gives a motor neuron command (R_n) consisting of a pulse, a slide, and a step.

The transfer function for the network shown in Fig. 10 is second order, having two factors in the numerator (zeros) and two in the denominator (poles). The overall transfer function of the final common path, obtained by cascading this neural network with a fourth-order plant, can give an approximation to the desired overall transfer function of $1/s$. Neglecting the high-frequency complex pole pair in the plant, the combined transfer function (E/V_c) is

$$\frac{s^2(BT_s) + s(AT_s + B + C) + A}{s(sT_s + 1)} \times \frac{(sT_z + 1)}{s^2(T_1T_2) + s(T_1 + T_2) + 1} \quad (1)$$

where T_z, T_1, T_2 represent the time constants in the plant's transfer function (factor on the right).

The zero in the plant dynamics can be compensated for by the pole in the neural network if $T_s = T_z$. In the model of normal saccades, the DC gain is one, which sets the value of A to one. The two zeros in the final common path can be used to compensate for two of the poles in the plant. Since T_s has already been fixed at T_z, we must choose the gain of the pulse as $B = T_1T_2/T_s$. The gain of the slide must then be $C = T_1 + T_2 - T_s - (T_1T_2/T_s)$. Hence, we can compensate for all the dynamics of the ocular motor plant (except the high-frequency, complex-pole pair, which, along with the dynamics of the pulse of innervation, will therefore determine the waveform of the saccade).

If the pulse, slide, and step components of innervation are not matched to the ocular plant, the eye will drift exponentially after the

rapid part of each saccade. An adaptive mechanism is presumed to exist that matches the parameters of the brain stem pathway postsaccadic retinal slip. Suppose that the gain of the step has been increased to suppress the postsaccadic retinal slip caused by our adaptation paradigm. If no other parameters were altered, the ocular drift that follows the end of the pulse-driven part of the saccade would have a very long time constant (due to the large plant time constant). Ocular drifts with longer time constants are produced by reductions in the amplitude of the slide, which shifts the time constant of the ocular drift toward the dominant time constant of the plant. To make ocular drifts with shorter time constants the amplitude of the slide must be increased. At some point (for ocular drifts with time constants of ~50 ms), however, further increases of the amplitude of the slide do not decrease the time constant of the ocular drift; instead they cause the eye to overshoot the final position (determined by the step) and drift back to it. To shorten the time constant of the ocular drift further therefore requires another mechanism. The simplest approach is to decrease the time constant of the neural slide component. By changing both the amplitude and the time constant of the slide it is possible to match time constants over the range of ocular drifts that we observed (~30–80 ms).

Simulation of spontaneous eye movements made in the dark

The above linear systems analysis suggests that the neural slide may be contributing to postsaccadic ocular drift. Individual eye-movement records from a monkey in both the normal and adapted states were simulated to evaluate the ability of the new model of the final common path to adequately reproduce actual eye movements. Simulation, of course, requires specification of more than just the final common path. The complete model of the saccadic system we used was very similar to one published earlier (42), with the exponen-

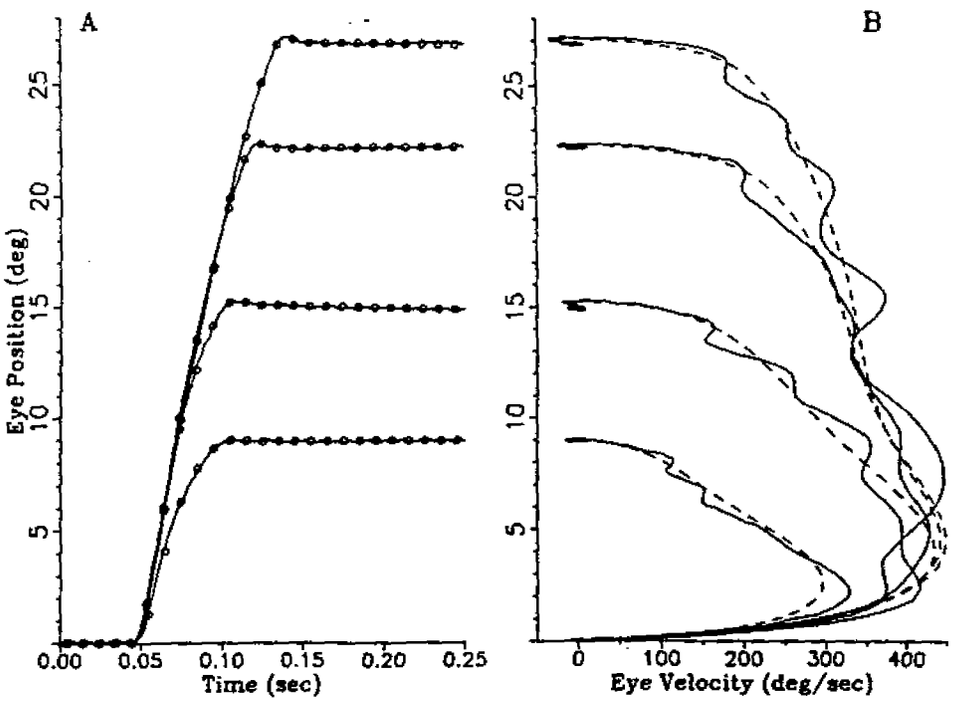

FIG. 11. Recordings and simulations of normal spontaneous saccades made in the dark. *A*: four individual eye movements from monkey OV were offset so that their initial positions were at zero. Superimposed on each data trace is a *dotted curve*, obtained by simulating the eye movement with a model based on the brain stem network shown in Fig. 10. *B*: eye position versus eye velocity phase plane. The eye-position values from the actual and simulated eye movement were differentiated with the same digital filter to obtain an eye-velocity signal. The phase-plane trajectories of the simulations (*dashed curves*) are superimposed on their corresponding data trajectories (*solid curves*). The fit is excellent for the beginning and ending (i.e., low-velocity portions) of the saccades.

tial burst-cell nonlinearity replaced by a power function, the brain stem network replaced by the one shown in Fig. 10, and with a fourth-order, lumped linear plant.

Figure 11 shows a family of spontaneous saccades made by monkey OV in the dark and simulated with the new model. Figure 11*A* shows four individual saccades of various amplitudes (offset to start at zero), and superimposed upon them, their four simulations (circles). (Model parameters were adjusted by hand to obtain a reasonable fit to the normal saccades.) The simulations and the eye movements are virtually identical. The fit of the model to the rapid part of the movement can be better appreciated in Fig. 11*B*, which plots each eye movement (solid curve) as a trajectory in the phase plane of eye position versus eye velocity. The simulations are shown as dashed curves. Comparison of the phase plane trajectories reveals that the model matches the eye movements closely, except for the oscillations in the eye velocity >100°/s. Since both the data and the simulated eye movements were processed with the same digital filter, the oscillations on the eye-velocity data indicate a true physiological phenomenon. This would be consistent with more detailed models of the ocular motor plant, which are of at least sixth order (4, 9, 35). Consideration of the higher-order terms in the plant will not be necessary for our study of the adaptive behavior of the saccadic system.

Two examples of spontaneous saccades in the dark from the range of ocular drift time constants are shown in Fig. 12 (τ_m is the time constant of the adapting image motion). Superimposed on the eye-movement traces are the corresponding simulated movements (circles). The fits are fairly good, except that in the simulation, after the pulse-driven part of the saccade is over, the overshoot of the plant (caused by the underdamped complex pole pair) always brings the eye to an almost complete stop before the ocular drift begins. Figure 12*A* shows that a saccade with a long time

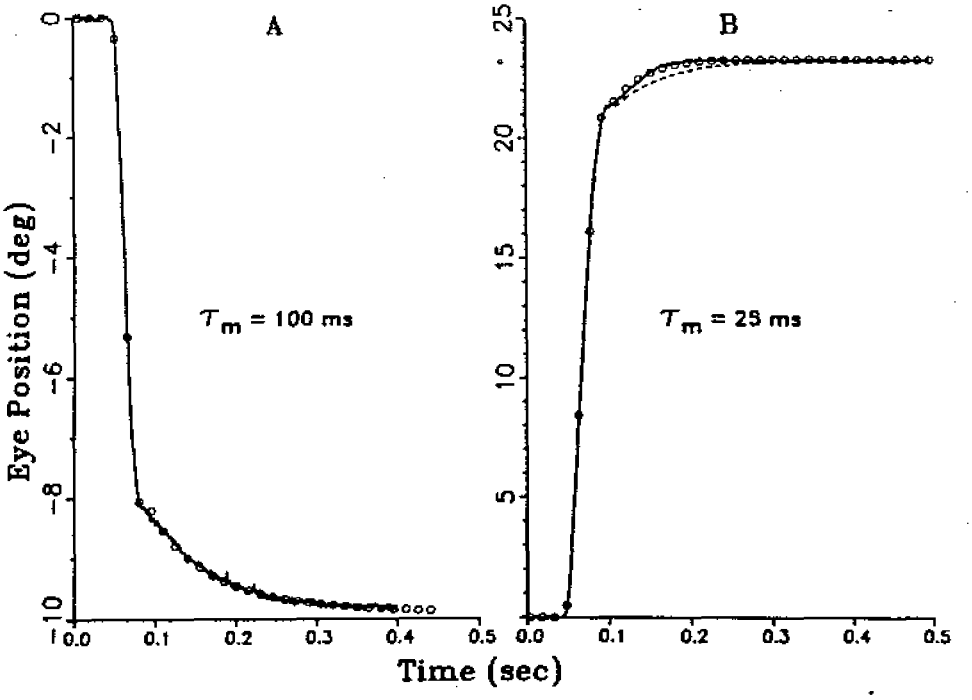

FIG. 12. Recordings and simulations of adapted spontaneous saccades made in the dark. Individual responses were chosen from monkey OV and offset to start from zero. *A*: eye movement (*solid curve*) and simulation (*circles*) after adaptation to exponential image slip with a time constant of 100 ms. The ocular drift has a time constant of ~80 ms. *B*: eye movement after adaptation to exponential image slip with a time constant of 25 ms. The ocular drift has a time constant of ~34 ms. The *dashed curve* is the best-fit simulation that can be obtained by changing only 2 elements: the gain of the step and the gain of the slide. The *circles* are the best fit that can be obtained by changing 3 elements: the gain of the step and both the gain and the time constant of the slide.

constant ocular drift (~80 ms) can be simulated by changing just the gain of the step and the slide components. Figure 12*B* shows that a saccade with a short time constant ocular drift (~34 ms) can not be simulated very well by changing just the step and slide gains (dashed curve). The model makes a good simulation of this eye movement, though, if the gain of the step and both the gain and the time constant of the slide can be adjusted (circles).

Adaptive control

The analytical discussion above, and the results of the simulation, demonstrate that both the step and slide components of ocular motor innervation are needed to describe the characteristics of postsaccadic ocular drift. The amplitude of the step of innervation and both the amplitude and the time constant of the neural slide need to be under adaptive control to compensate for changes in ocular motor strength and to exactly cancel the equivalent zero in the plant dynamics. Since the effect of the newly proposed pole in the brain stem network is to hide the zero of the plant neither the pole nor the zero have been taken into account in previous studies of the saccadic system. However, we now suggest that the suppression of postsaccadic ocular drift is achieved by adaptively changing three elements: the gain of the step of innervation and both the gain and the time constant of the slide of innervation. This detailed understanding of the nature of the adaptive changes in the brain stem pathways makes it possible to study the interaction between this part of the saccadic system and other ocular motor systems. Since the new branch (bottom of Fig. 10) is needed to compensate for the zero in the plant dynamics, it should be shared by all ocular motor systems, thereby justifying its inclusion in the final common path, rather than relegating it to the saccadic system alone. This shared role may be tested experimentally by measuring the performance of other ocular motor systems before and after adaptation of the saccadic system to persistent postsaccadic retinal slip.

ACKNOWLEDGMENTS

We are grateful for the assistance of Dr. Kenji Kawano in measuring the latencies of the ocular following responses. We thank Dr. Herschel Goldstein for many helpful discussions about the pulse-slide-step firing patterns of abducens neurons. We are grateful to Dr. Lawrence Stark for suggesting the use of the least-upper-bound to characterize the main sequence data.

Partial support for L. M. Optican was provided by National Eye Institute Fellowship EY-05291.

Received 4 October 1984; accepted in final form 10 May 1985.

REFERENCES

1. ABEL, L. A., SCHMIDT, D., DELL'OSSO, L. F., AND DAROFF, R. B. Saccadic system plasticity in humans. *Ann. Neurol.* 4: 313–318, 1978.
2. BAHILL, A. T., CLARK, M. R., AND STARK, L. The main sequence, a tool for studying human eye movements. *Math. Biosci.* 24: 191–204, 1975.
3. BAHILL, A. T., CLARK, M. R., AND STARK, L. Glissades—eye movements generated by mismatched components of the saccadic motoneuronal control signal. *Math. Biosci.* 26: 303–318, 1975.
4. BAHILL, A. T., LATIMER, J. R., AND TROOST, B. T. Linear homeomorphic model for human eye movement. *IEEE Trans. Biomed. Eng.* 27: 631–639, 1980.
5. BAKER, R., PRECHT, W., AND LLINÁS, R. Mossy and climbing fiber projections of extraocular muscle afferents to the cerebellum. *Brain Res.* 38: 440–445, 1972.
6. COHEN, B. AND HENN, V. Unit activity in the pontine reticular formation associated with eye movements. *Brain Res.* 46: 403–410, 1972.
7. COLLINS, C. C., O'MEARA, D., AND SCOTT, A. B. Muscle tension during unrestrained human eye movements. *J. Physiol. London* 245: 351–369, 1975.
8. DEUBEL, H., WOLF, W., AND HAUSKE, G. Corrective saccades: effect of shifting the saccade goal. *Vision Res.* 22: 353–364, 1982.
9. ENDERLE, J. D., WOLFE, J. W., AND YATES, J. T. The linear homeomorphic saccadic eye movement model—a modification. *IEEE Trans. Biomed. Eng.* 31: 717–720, 1984.
10. FUCHS, A. F. AND KORNHUBER, H. H. Extraocular muscle afferents to the cerebellum of the cat. *J. Physiol. London* 200: 713–722, 1969.
11. FUCHS, A. F. AND LUSCHEI, E. S. Firing patterns of abducens neurons of alert monkeys in relationship to horizontal eye movement. *J. Neurophysiol.* 33: 382–392, 1970.
12. GISBERGEN, J. A. M. VAN, ROBINSON, D. A., AND GIELEN, S. A quantitative analysis of generation of saccadic eye movements by burst neurons. *J. Neurophysiol.* 45: 417–442, 1981.
13. GOLDSTEIN, H. P. *The Neural Encoding of Saccades in the Rhesus Monkey* (PhD thesis). Baltimore, MD: Johns Hopkins Univ., 1983.
14. HENSON, D. B. Corrective saccades: effect of altering visual feedback. *Vision Res.* 18: 63–67, 1979.
15. JUDGE, S. J., RICHMOND, B. J., AND CHU, F. C. Implantation of magnetic search coils for measurement of eye position: an improved method. *Vision Res.* 20: 535–538, 1980.
16. KAWANO, K. AND MILES, F. A. Adaptive plasticity in short-latency ocular following responses of monkey. *Soc. Neurosci. Abstr.* 9: 868, 1983.
17. KELLER, E. L. Participation of medial pontine reticular

formation in eye movement generation in monkey. *J. Neurophysiol.* 37: 316–332, 1974.
18. KELLER, E. L. AND ROBINSON, D. A. Absence of a stretch reflex in extraocular muscles of the monkey. *J. Neurophysiol.* 34: 908–919, 1971.
19. KOMMERELL, G., OLIVIER, D., AND THEOPOLD, H. Adaptive programming of phasic and tonic components in saccadic eye movements. Investigations in patients with abducens palsy. *Invest. Ophthalmol.* 15: 657–660, 1976.
20. LEIGH, R. J. AND ZEE, D. S. *The Neurology of Eye Movements.* Philadelphia, PA: Davis, 1983, p. 215–216.
21. MARQUARDT, D. W. An algorithm for least-squares estimation of nonlinear parameters. *J. SIAM* 11: 431–441, 1963.
22. MIYASHITA, Y. Eye velocity responsiveness and its proprioceptive component in the floccular Purkinje cells of the alert pigmented rabbit. *Exp. Brain Res.* 55: 81–90, 1984.
23. OPTICAN, L. M. Saccadic dysmetria. In: *Functional Basis of Ocular Motility Disorders,* edited by G. Lennerstrand, D. S. Zee, and E. L. Keller. Oxford, UK: Pergamon, 1982, p. 441–451.
24. OPTICAN, L. M., FRANK, D. E., SMITH, B. M., AND COLBURN, T. R. An amplitude and phase regulating magnetic field generator for an eye movement monitor. *IEEE Trans. Biomed. Eng.* 29: 206–209, 1982.
25. OPTICAN, L. M. AND MILES, F. A. Visually induced adaptive changes in oculomotor control signals. *Soc. Neurosci. Abstr.* 5: 380, 1979.
26. OPTICAN, L. M. AND ROBINSON, D. A. Cerebellar-dependent adaptive control of primate saccadic system. *J. Neurophysiol.* 44: 1058–1076, 1980.
27. OPTICAN, L. M., ZEE, D. S., MILES, F. A., AND LISBERGER, S. G. Oculomotor deficits in monkeys with floccular lesions. *Soc. Neurosci. Abstr.* 6: 474, 1980.
28. POLA, J. AND ROBINSON, D. A. Oculomotor signals in medial longitudinal fasciculus of the monkey. *J. Neurophysiol.* 41: 245–259, 1978.
29. RABINER, L. R. AND GOLD, B. *Theory and Application of Digital Signal Processing.* Englewood Cliffs, NJ: Prentice-Hall, 1975, chapt. 3.
30. ROBINSON, D. A. A method of measuring eye movement using a scleral search coil in a magnetic field. *IEEE Trans. Biomed. Eng.* 26: 137–145, 1963.
31. ROBINSON, D. A. The mechanics of human saccadic eye movement. *J. Physiol. London* 174: 245–264, 1964.
32. ROBINSON, D. A. The mechanics of human smooth pursuit eye movement. *J. Physiol. London* 180: 569–591, 1965.
33. ROBINSON, D. A. A note on the oculomotor pathway. *Exp. Neurol.* 22: 130–132, 1968.
34. ROBINSON, D. A. Oculomotor unit behavior in the monkey. *J. Neurophysiol.* 33: 393–404, 1970.
35. ROBINSON, D. A. Models of mechanics of eye movements. In: *Models of Oculomotor Behavior and Control,* edited by B. L. Zuber. Boca Raton, FL: CRC Press, 1981, p. 21–41.
36. ROBINSON, D. A. AND KELLER, E. L. The behavior of eye movement motoneurons in the alert monkey. *Bibl. Ophthalmol.* 82: 7–16, 1972.
37. SCHWARZ, D. W. F. AND TOMLINSON, R. D. Neuronal responses to eye muscle stretch in cerebellar lobule VI of the cat. *Exp. Brain Res.* 27: 101–111, 1977.
38. SHRAGER, R. I. Nonlinear regression with linear constraints: an extension of the magnified diagonal method. *JACM* 17: 446–452, 1970.
39. SKAVENSKI, A. A. AND ROBINSON, D. A. Role of abducens neurons in vestibuloocular reflex. *J. Neurophysiol.* 36: 724–738, 1973.
40. WEBER, R. B. AND DAROFF, R. B. Corrective movements following refixation saccades: type and control system analysis. *Vision Res.* 12: 467, 1972.
41. WOLF, W., DEUBEL, H., AND HAUSKE, G. Properties of parametric adjustment in the saccadic system. In: *Theoretical and Applied Aspects of Eye Movement Research,* edited by A. G. Gale and F. Johnsons. Amsterdam: Elsevier/North-Holland, 1984, p. 79–86.
42. ZEE, D. S., OPTICAN, L. M., COOK, J. D., ROBINSON, D. A., AND ENGEL, W. K. Slow saccades in spinocerebellar degeneration. *Arch. Neurol.* 33: 243–251, 1976.